ELSEVIER

Journal of Photochemistry and Photobiology A: Chemistry 101 (1996) 1–5

Journal of PHOTOCHEMISTRY AND PHOTOBIOLOGY A: CHEMISTRY

ArF laser dissociation of trisilane

Rosa Becerra [a], Milagros Ponz [b], Marta Castillejo [a], Mohamed Oujja [a], Javier Ruiz [a,1], Margarita Martin [a,*]

[a] *Instituto de Química Física "Rocasolano", C.S.I.C., Serrano 119, 28006 Madrid, Spain*

[b] *Facultad de Ciencias Experimentales y Técnicas, Universidad San Pablo CEU, 28660 Boadilla del Monte, Spain*

Received 17 April 1996; accepted 3 June 1996

Abstract

The laser photolysis of trisilane at 193 nm was studied. The final photolysis products were monosilane, disilane and tetrasilanes. The results were indicative of the participation in the photolysis process of at least two different dissociation pathways which account for about 80% of the total parent molecule dissociation. ArF laser multiphoton dissociation of Si_3H_8 in a free jet expansion was also studied. Photofragment fluorescence from $SiH(A^2\Delta)$ and several singlet and triplet excited states of the silicon atom was observed. The rovibrational population distributions in $SiH(A^2\Delta)$ were obtained by spectral simulation. The rotational distributions can be characterized by near-Boltzmann distributions. The average rotational energies in $v=0$ and $v=1$ are 1550 and 1140 cm^{-1} respectively and the average vibrational energy in the observed vibrational levels ($v=0$–2) is 800 cm^{-1}.

Keywords: Laser photolysis; Photofragment fluorescence; Trisilane

1. Introduction

The smallest stable silicon hydrides, silane and disilane, have been the subject of photochemical and spectroscopic studies [1–3]. In recent work, the role of stable silicon hydrides as photochemical sources of silicon hydride radicals and other relevant information on their kinetic properties and thermochemistry have been reviewed [4]. A knowledge of the photofragmentation channels of silanes is of importance in order to understand and control the chemical vapour deposition of silicon thin films. Moreover, new transient silicon hydride species, some still uncharacterized, are expected to be formed as primary dissociation products [2]. In addition, experimental evidence has indicated that certain selective processes may take place in the photodissociation of silanes. In the vacuum UV photodissociation of monosilane, the only silicon-containing products observed are Si atoms and electronically excited silylidyne [1]. In the photolysis of disilane, $SiH(A^2\Delta)$ is formed promptly; however, ground state $SiH(X^2\Pi)$ cannot be observed within approximately 100 ns after the photolysis pulse [5].

For the next stable silicon hydride, Si_3H_8, the onset of absorption shifts towards longer wavelengths with respect to monosilane and disilane [3]. UV photolysis of Si_3H_8 has been reported to be a source of SiH_2 [4,6], but little information about other photodissociation processes is available. In this work, we have undertaken a study of the ArF laser photolysis of trisilane. We report our initial results on the single-photon photolysis processes, and the observation of several excited photofragments following laser multiphoton dissociation of trisilane.

2. Experimental details

The experimental set-up was similar to that used in previous work [7]. Samples of trisilane kept in a slush bath at −15 °C were expanded into a vacuum chamber through a pulsed solenoid valve (General Valve Corporation; diameter, 0.5 mm; typically operated at a pulsed voltage of approximately 60 V and approximately 300 μs). About 10 mm below the nozzle the molecular beam was perpendicularly crossed by the output of an ArF laser. The laser beam was focused approximately 40 cm behind the interaction region. Photofragment fluorescence produced in the interaction region was imaged by a lens onto the entrance slit of a 0.5 m monochromator and the dispersed fluorescence was viewed by a photomultiplier (Hamamatsu R928). The time-integrated photomultiplier signals were fed to SRS245 gated integrators

* Corresponding author. Tel.: +34 1 561 94 00; fax: +34 1 564 24 31.

[1] Present address: Departamento de Física Aplicada, Facultad de Ciencias, Universidad de Málaga, Spain.

PII S1010-6030(96)04427-9

and boxcar averagers and sent to an analogue to digital converter built in to a programmable unit, which also allowed control of the laser and valve trigger pulses and the monochromator wavelength scan. The digitized signals were transferred to a microcomputer.

Experiments were also performed to determine the final products after photolysis at 193 nm. In these experiments, the laser output was coupled into a glass cell equipped with quartz windows and the products were analysed by gas chromatography (GC). Typical analyses of the product mixtures were carried out using a Hewlett Packard 5890 chromatograph equipped with a flame ionization detector. A 4 m PS-255 column with N_2 carrier gas was operated at 50 °C for 10 min and then the temperature was raised to 90 °C. Retention times were characterized with authentic samples.

Samples of trisilane were analysed by GC–mass spectrometry, showing a purity better than 99%.

3. Results and discussion

3.1. Final dissociation products

Indirect evidence concerning the primary photofragmentation processes was sought through GC analysis of the final dissociation products. In order to obtain sufficient decomposition products, samples of 0.5 Torr of trisilane were photolysed by 100 laser shots. Experiments were carried out under two different laser beam focusing conditions, corresponding to the same laser energy (approximately 8 mJ at the entrance of the photolysis cell) and fluences of 30 mJ cm^{-2} and 200 mJ cm^{-2}.

The major photolysis products were SiH_4 and Si_2H_6. The relative yield of monosilane was about 1.3 times that of disilane for both laser focusing conditions. At the lower fluence, smaller proportions of tetrasilanes, i-Si_4H_{10} and n-Si_4H_{10}, were also found (not observed at the higher laser fluence). The formation of solid deposits, observed in both cases, was much more prominent at the higher fluence. Low and high laser fluence experiments yielded similar amounts of monosilane, although the relative decomposition of the parent molecule increased about four times with increasing laser fluence. Under the low laser fluence conditions, the dissociation pathways leading to monosilane and disilane yielded about 80% of the total trisilane decomposition, suggesting that other dissociation pathways, second ArF laser photon absorption processes and secondary reactions with the parent compound constitute minor but non-negligible contributions to the total decomposition of trisilane. Some of the latter contributions increased at higher laser fluences. The formation of radical species in secondary processes, which may undergo effective reactions with the parent molecule, may be responsible for the enhanced depletion of trisilane.

The results at low fluence can be understood in the light of photochemical processes and reaction mechanisms identified in the chemistry of other silicon hydrides [6,8,9]. The participation of two different photodissociation channels can be inferred: in the first, the observed monosilane is produced together with the transient species H_3SiSiH; in the second, the primary products are the observed disilane and $SiH_2(X^1A_1)$ which, in turn, is effectively inserted into the Si–H bond of the parent molecule [4] leading to tetrasilanes as final products. The relative weight of each dissociation channel can be estimated from the relative yields of monosilane to disilane. The error in this estimation, due to a certain amount of decomposition of disilane by ArF laser dissociation, is expected to be small as the absorption coefficients at 193 nm are about ten times smaller for disilane than for trisilane [3]. With regard to the minor contributions to the one-photon trisilane dissociation, fragmentation of trisilane into silyl and Si_2H_5 radicals is allowed on energy grounds; however, the detection of silyl by the identification of products resulting from the reaction of silyl with the parent molecule is precluded due to its lack of rapid reaction with most closed shell molecules (rate constants four orders of magnitude slower than for reactions of SiH_2) [4,8]. Therefore the participation of the dissociation channel leading to silyl radicals cannot be excluded; however, it is unlikely that 20% of the photodecomposition of trisilane, not accounted for by the analysed final products, can be attributed to silyl radicals. Most of the decomposed trisilane missing in the mass balance may be present in the form of solid deposits observed in the dissociation process.

3.2. Observed photofragment emission

In the spectral region from 200 to 400 nm, emission from several electronically excited states of the Si atom was recorded. The atomic states responsible for the most intense emissions were the triplets $4s^3P^0$ and $3p^3D^0$ and the singlet $3d^1D^0$. In Table 1, the energies, relative spectral intensities and estimated relative populations of the assigned atomic states are given. A very weak emission near 380 nm can be

Table 1
Estimated relative populations of the excited states of Si observed following ArF laser dissociation of trisilane

Observed state	Energy (cm^{-1})	Relative spectral intensity [d]	Estimated relative population [e]
$Si(4s^3P^0_{2,1,0})$	39955.16 [a]	0.6	0.3 ± 0.2
$Si(4s^1P^0_1)$	40991.88	0.1	0.03 ± 0.02
$Si(3p^3D^0_{3,2,1})$	45293.629[b]	1	
$Si(3d^1D^0_2)$	47351.55	0.3	1
$Si(3d^3F^0_{2,3,4})$	49933.778[c]	< 0.01	
$Si(3d^1F^0_3)$	53362	0.6	0.20 ± 0.05
$Si(3d^1P^0_1)$	53387	< 0.01	< 0.006

[a,b,c] Energy of components $J=2$, $J=2$ and $J=3$ respectively.

[d] Intensities have been divided by a reference linearly dependent on the laser energy and corrected for the spectral response of the monochromator/photomultiplier.

[e] Relative populations have been estimated as described in Ref. [10].

assigned to the band sequence $v' - v'' = 1$ of the $SiH(A^2\Delta \rightarrow X^2\Pi)$ system. The strong emission between 400 and 600 nm is readily assigned to the band sequence $v' - v'' = 0$ of the $SiH(A^2\Delta \rightarrow X^2\Pi)$ transition.

On energy grounds, two ArF laser photons are required to produce $SiH(A^2\Delta)$ from the parent molecule. With regard to the excited states of atomic silicon, there are several two-photon dissociation processes energetically and spin allowed leading to the assigned singlets and lowest lying triplets listed in Table 1. Formation of the triplets $3p^3D$ and $3d^3F$, giving rise to strong and weak emission signals respectively, requires absorption of at least three photons if the spin is to be conserved in the dissociation.

In order to confirm the order of the absorption processes, the dependence of the $SiH(A^2\Delta)$ and $Si(4s^3P^0)$ photofragments on the laser energy was studied. The best fit to a straight line of the logarithmic plot of the fluorescence signal vs. the laser energy gave slopes of 1.2 and 1.6 for the $SiH(A^2\Delta)$ and $Si(4s^3P^0)$ signals respectively, probably indicating that a certain step in the absorption process is saturated.

At 193 nm, trisilane is excited to the first molecular Rydberg state. If the lifetime of this state is in the picosecond range, at the laser power of about 10^{26} photons cm^{-2} s^{-1} used in the present experiments, and assuming that the cross-section for absorption of a second ArF laser photon is approximately 10^{-17} cm^2 (typical for an allowed transition), a moderately high yield of 0.001 for the second photon absorption process can be estimated. The possible dissociation products thermochemically allowed if an energy equivalent to two ArF laser photons were added to the parent molecule are listed in Table 2. The total energy available to the products for each possible two-photon process has been calculated using recent thermochemical values of the heats of formation of the reactants and products [4,8,9,11–13].

A second laser photon absorption by the primary photofragments formed after one-photon dissociation of trisilane may also lead to the observed photofragment emission. With regard to the stable species SiH_4 and Si_2H_6, only the latter is known to absorb at 193 nm, although the formation of $SiH(A^2\Delta)$ or excited silicon atoms is not energetically possible by ArF laser absorption of disilane in the ground state. Therefore only the fraction of disilane formed during the primary dissociation with an excess energy of at least about 20 000 cm^{-1} could participate in the possible second photon process. The same thermochemical arguments apply to $SiH_2(X^1A_1)$, although in this case only an excess energy of about 100 cm^{-1} is the minimum required to make the process available. However, no singlet silylene states are predicted to lie in the energy region which could be excited by a second ArF laser photon [14] and the above dissociation pathway will not be considered in this work. Laser absorption at 193 nm by the transient species H_3SiSiH and SiH_3 may, on energetic grounds, lead to the formation of excited silylidyne. For H_3SiSiH, broad-band absorptions between 330 and 365 nm have been tentatively assigned [2], but no information is available about absorption at shorter wavelengths. ArF laser absorption by the silyl radical has not been established, but experimental and theoretical evidence indicates the presence of a Rydberg state lying in the energy region which may be reached on 193 nm excitation [15,16]; on the other hand, dissociation of silyl into SiH and H_2 has been suggested to occur in the vacuum UV dissociation of silane [1]. Despite this, as discussed in the previous section, its formation in the dissociation of trisilane at 193 nm cannot be either disregarded or confirmed from the evidence obtained in this work, thus making uncertain its possible participation in the second photon absorption process.

Table 2
Two-photon ArF laser excitation of trisilane. Spin-allowed, energetically available [a] dissociation channels leading to $SiH(A^2\Delta)$ and excited silicon atoms

Channel	Possible dissociation products	Available energy (cm^{-1}) [a]
I	$SiH(A^2\Delta) + SiH_4 + SiH_3(X^2A_1)$	37820
II	$SiH(A^2\Delta) + Si_2H_6 + H(^2S)$	32231
III [b]	$SiH(A^2\Delta) + SiH_4 + SiH_2(X^1A_1) + H(^2S)$	13222
IV [c]	$SiH(A^2\Delta) + Si_2H_{2x} + (3-x)H_2 + H$ $(x=1,2)$	[d]
V	$SiH(A^2\Delta) + Si_2H_{2x+1} + (3-x)H_2$ $(x=0–2)$	[e]
	$Si(4s^1P^0_1) + SiH_4 + SiH_4$	30072
	$Si(3d^1D^0_2) + SiH_4 + SiH_4$	22713
	$Si(3d^1F^0_3) + SiH_4 + SiH_4$	16702
	$Si(3d^1P^0_1) + SiH_4 + SiH_4$	16677
	$Si(4s^1P^0_1) + Si_2H_{2x} + (4-x)H_2$	[f]
	$Si(3d^1D^0_2) + Si_2H_6 + H_2$	21768
	$Si(3d^1F^0_3) + Si_2H_6 + H_2$	15758
	$Si(3d^1P^0_1) + Si_2H_6 + H_2$	15733
	$Si(4s^1P^0_1) + SiH_3 + SiH_3 + H_2$	1288
	$Si(4s^3P^0_2) + SiH_4 + SiH_2(a^3B_1) + H_2$	2816
	$Si(4s^3P^0_2) + SiH_3 + SiH_3 + H_2$	2325

[a] Heats of formation for the different species involved are taken from experimental estimations [4,8,9,11–13].
[b] Via either an excited state of the parent molecule or secondary absorption and dissociation of SiH_2. Formation of triplet silylene is also allowed.
[c] Via either an excited state of the parent molecule or secondary absorption and dissociation of SiH_3.
[d] For $x=1$, E_{avail} is 6803 cm^{-1}; for $x=2$, E_{avail} can be estimated as 10 858 or 13 292 cm^{-1} depending on the isomeric form of Si_2H_4.
[e] For $x=0$, 1 and 2, E_{avail} values are estimated as 15 862, 23 452 and 38 807 cm^{-1} respectively.
[f] For $x=1$, 2 and 3, E_{avail} values are estimated as 2647, 6855 and 28 128 cm^{-1} respectively.

3.3. Rovibrational population distribution in $SiH(A^2\Delta)$

In order to gain some insight into the formation mechanisms leading to $SiH(A^2\Delta)$, we have performed spectral simulation calculations to obtain the rovibrational population distributions in the observed $SiH(A^2\Delta)$ photofragment. The method has been described elsewhere [17]. Spectroscopic constants for silylidyne were taken from Herzberg et al. [18]. Transition energies for the emission bands $v' = 0 \rightarrow v'' = 0$, $v' = 1 \rightarrow v'' = 1$ and $v' = 2 \rightarrow v'' = 2$ were taken from the literature [19,20]. Rovibronic transition energies not included in

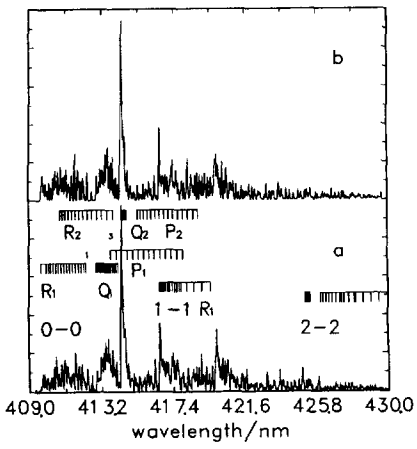

Fig. 1. (a) SiH($A^2\Delta \rightarrow X^2\Pi$) emission spectrum recorded following ArF laser dissociation of a free jet of trisilane. Spectral resolution is 0.048 nm. The spectrum has been corrected for the response of the monochromator/photomultiplier and for shot-to-shot laser fluctuations. Each point is the average of 20 laser shots. (b) Spectrum simulated with the vibrational and rotational distributions obtained by the algorithm described in Ref. [17]. The assignment for the $v''=0 \leftarrow v'=0$ transition has been taken from Ref. [20]. For transitions from $v'=1$ and $v'=2$, only the onsets of the bands are indicated.

the tabulated values of the above references and the transition probabilities were calculated as described in Ref. [17].

Experimental and calculated spectra are shown in Fig. 1. The rotational populations obtained from the spectral simulation calculations for levels $v=0$ and 1 can be well fitted by Boltzmann-type distributions. In Fig. 2, the rotational populations of $v=0$ and 1 are represented in Boltzmann plots. The average rotational energies in $v=0$ and $v=1$ are approximately 1550 cm^{-1} and 1140 cm^{-1} respectively; the average energy appearing as the vibrational energy calculated considering the populations obtained for $v=0$–2 is approximately 800 cm^{-1}.

Product rotational populations, which can be characterized by near-Boltzmann distributions, are indicative of a dissociation process which occurs on a time scale of sufficient length to permit energy transfer and equilibration of fragment rotation. In this case, the dissociation process can be described by statistical theories [21]. In the following section, we show the results of application of the prior model [22,23] to the possible dissociation channels leading to SiH($A^2\Delta$).

3.4. Prior calculations

The prior rotational and vibrational distributions for SiH($A^2\Delta$, $v=0$–2) were calculated for the two-photon dissociation channels numbered I–III listed in Table 2. Calculations were also performed for one of the stepwise mechanisms discussed in Section 3.2: dissociation of trisilane into SiH_3 and Si_2H_5, followed by second photon absorption and dissociation of silyl into SiH($A^2\Delta$) and molecular hydrogen.

Starting from the prior distribution of states in the products, the distribution in the rotational and vibrational degrees of

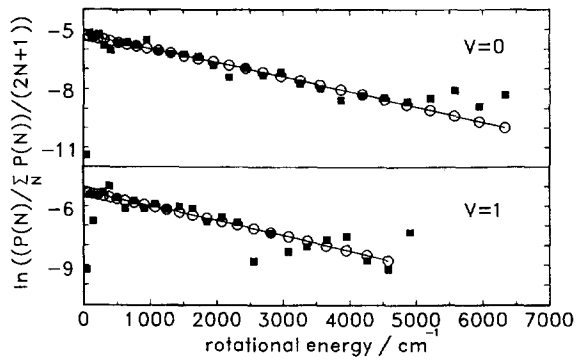

Fig. 2. Boltzmann plots of the rotational populations for $v=0$ and 1 obtained from the experimental emission spectrum shown in Fig. 1 (■); the full lines connecting the symbols ○ are the rotational prior distributions calculated for dissociation channel II (see text).

freedom of SiH($A^2\Delta$) were obtained by integrating or performing a discrete summation over all other degrees of freedom of the products [22,23]. The rotational and vibrational energies of fragments containing more than three atoms and the relative translational energies were treated as continuous variables, whereas for diatomic products, such as H_2, rotational and vibrational energies were calculated from known spectroscopic constants [24]. The vibrational energy of $SiH_2(X^1A_1)$ was also treated in the summation as a discrete variable and was calculated using recently reported vibrational constants [25,26].

The prior rotational distributions in SiH($A^2\Delta$) which best fit the rotational experimental populations are obtained when the calculation is applied to the dissociation channel leading to disilane and a hydrogen atom as final products (channel II in Table 2). In Fig. 2, Boltzmann plots of the prior distributions calculated for dissociation channel II are compared with the rotational populations obtained from the experimental spectrum. The average vibrational energy calculated from the prior vibrational distribution (calculated for levels $v=0$–2 in SiH($A^2\Delta$)) is 600 cm^{-1}, in moderate agreement with that obtained from the experimental vibrational populations. For the more exoergic dissociation channel I, the prior calculations lead to rovibrational distributions slightly hotter than, but rather similar to, those obtained for channel II, whereas for the less exothermic channel III, distributions colder than the experimental values are obtained.

In the stepwise mechanism involving the silyl radical, the prior calculation, applied to the first photon dissociation of trisilane, leads to an average vibrational energy in silyl of about 6100 cm^{-1}. The energy available to SiH($A^2\Delta$) and H_2 in the second photon dissociation of silyl was estimated by adding this value to the exothermicity of the second photon dissociation process. The prior calculations lead to population distributions in SiH($A^2\Delta$) significantly hotter than the experimental values.

4. Final discussion and conclusions

In the one-photon dissociation of trisilane at 193 nm, two major dissociation channels have been identified. In both

dissociation pathways, formation of the observed final products involves the breaking of one Si–Si bond, followed by rearrangement and secondary reactions of the fragments. This is consistent with spectroscopic studies which assign the trisilane absorption band near 190 nm to a Rydberg transition from a $3b_2$ orbital (largely representing σ_{SiSi} bonds [3]) to a 4s orbital. Although the dissociation channel leading to silyl radicals will require a minimum rearrangement of the atoms, it has not been observed; its participation in photolysis, as a minor dissociation pathway, is unlikely, but cannot be completely ruled out.

Formation of electronically excited silicon atoms and silylidyne is also observed following ArF laser excitation. The high relative population of the observed singlets $3d^1D$ and $3d^1F$ is compatible with the availability of highly exoergic spin-allowed two-photon dissociation pathways. However, the $3d^1P$ state has a relative population two orders of magnitude smaller than the $3d^1D$ state despite the similar possible dissociation channels available to it. Moreover, the $3d^3D$ state, for which no spin-allowed dissociation pathways are open at the energy of two ArF laser photons, is observed with relatively high intensity. This suggests that spin-forbidden or three-photon absorption processes may be relatively important in explaining the observed excited silicon atom distribution.

With regard to the mechanisms leading to $SiH(A^2\Delta)$, some tentative conclusions can be drawn. The near-Boltzmann rotational distribution in excited silylidyne indicates that the fragment is formed via a statistical dissociation pathway. The prior rovibrational distributions in $SiH(A^2\Delta)$ best approaching the experimental populations are obtained when the calculation is applied to the most exoergic two-photon dissociation channels. This is expected because polyatomic cofragments accompany the formation of excited silylidyne, and only a small fraction of the available energy can be channelled into the internal energy of $SiH(A^2\Delta)$. For the stepwise mechanism involving a second photon absorption of $SiH_3(X^2A_1)$, the situation is reversed, as the cofragment of excited silylidyne in the dissociation is the hydrogen molecule. Thus, although the energy available to the products is smaller than for the pathways referred to above, a larger fraction of the energy goes into the rotation and vibration of $SiH(A^2\Delta)$, leading to distributions hotter than the experimental populations.

Acknowledgements

Financial support from the Spanish DGICYT (PB93-0145-CO2-01), Universidad San Pablo-CEU (project no. 13/95) and the Human Capital and Mobility Programme of the European Community (CHRX-CT94-0485) is acknowledged. Thanks are also due to Dr. Frank Slootman (L'Air Liquide) for arranging the gift of a sample of trisilane.

References

[1] Th. Glenewinkel-Meyer, J.A. Bartz, G.M. Thorson and F.F. Crim, *J. Chem. Phys., 99* (1993) 5944.
[2] J.M. Jasinski, *Chem. Phys. Lett., 183* (1991) 558.
[3] U. Itoh, Y. Toyoshima, H. Onuki, N. Washida and T. Ibuki, *J. Chem. Phys., 85* (1986) 4867.
[4] J.M. Jasinski, R. Becerra and R. Walsh, *Chem. Rev., 95* (1995) 1203.
[5] M.H. Begemann, R.W. Dreyfus and J.M. Jasinski, *Chem. Phys. Lett., 155* (1989) 351.
[6] R. Becerra, H.M. Frey, B.P. Mason and R. Walsh, *J. Organomet. Chem.*, accepted for publication.
[7] J. Ruiz and M. Martin, *Chem. Phys. Lett., 226* (1994) 300.
[8] R. Becerra and R. Walsh, *J. Phys. Chem., 91* (1987) 5765.
[9] R. Becerra and R. Walsh, *J. Phys. Chem., 96* (1992) 10 856.
[10] M. Oujja, M. Martin, R. de Nalda and M. Castillejo, *Laser Chem., 16* (1996) 157.
[11] R. Walsh, *Acc. Chem. Res., 14* (1981) 246.
[12] R. Becerra, H.M. Frey, B.P. Mason, R. Walsh and M.S. Gordon, *J. Chem. Soc., Faraday Trans., 91* (1995) 2723.
[13] B. Ruscic and J. Berkowitz, *J. Chem. Phys., 95* (1991) 2416.
[14] B. Wirsam, *Chem. Phys. Lett., 14* (1972) 214.
[15] R.D. Johnson III and J.W. Hudgens, *Chem. Phys. Lett., 141* (1987) 163.
[16] G. Olbrich, *Chem. Phys., 101* (1986) 381.
[17] J. Ruiz and M. Martin, *Comp. Chem., 19* (1995) 417.
[18] G. Herzberg, A. Lagerqvist and B.J. McKenzie, *Can. J. Phys., 47* (1969) 1889.
[19] A.E. Douglas, *Can. J. Phys., 35* (1957) 71.
[20] G.D. Rochester, *Z. Phys., 101* (1936) 769.
[21] D.J. Nesbitt, H. Petek, M.F. Foltz, S.V. Filseth, D.J. Bamford and C.B. Moore, *J. Chem. Phys., 83* (1985) 223.
[22] A. Ben-Shaul, Y. Haas, K.L. Kompa and R.D. Levine, *Lasers and Chemical Change*, Springer Series in Chemical Physics 10, Springer-Verlag, Berlin, Heidelberg, New York, 1981, p. 177.
[23] E. Zamir and R.D. Levine, *Chem. Phys., 52* (1980) 253.
[24] G. Herzberg, *Molecular Spectra and Molecular Structure. I. Spectra of Diatomic Molecules*, Van Nostrand Reinhold, New York, 1950, p. 530.
[25] H. Ishikawa and O. Kajimoto, *J. Mol. Spectrosc., 160* (1993) 1.
[26] H. Ishikawa and O. Kajimoto, *J. Mol. Spectrosc., 174* (1995) 270.